Heliyon 9 (2023) e20716

Contents lists available at ScienceDirect

Heliyon

journal homepage: www.cell.com/heliyon

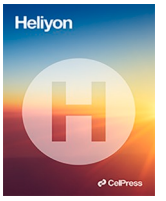

Apoptotic bodies of bone marrow mesenchymal stem cells inhibit endometrial stromal cell fibrosis by mediating the Wnt/β-catenin signaling pathway

Zhenghua Xiong [a,b,1], Yaru Ma [c,1], Jia He [d,1], Qin Li [b], Liu Liu [d], Chunli Yang [e], Jia Chen [b], Yi Shen [b], Xuesong Han [a,b,*]

[a] Department of Gynecology, First Affiliated Hospital of Kunming Medical University, Kunming, Yunnan, China
[b] Department of Gynecology, Yan'an Hospital Affiliated to Kunming Medical University, Kunming, Yunnan, China
[c] Department of Gynecology, Women and Children's Hospital Affiliated to Qingdao University, Qingdao, Shandong, China
[d] Department of Plastic Surgery, Affiliated Calmette Hospital of Kunming Medical University, Kunming, Yunnan, China
[e] Department of Gynecology, Baoshan People's Hospital, Baoshan, Yunnan, China

ARTICLE INFO

Keywords:
Endometrial stromal cells
Bone marrow mesenchymal stem cells
Apoptotic body
Fibrosis
Wnt/β-catenin signaling pathway

ABSTRACT

Background: Intrauterine adhesions (IUAs) are a common illness of the uterine cavity. Endometrial fibrosis is the main pathological feature. In addition to a high recurrence rate, patients with severe IUAs have a low pregnancy rate. However, there are few effective treatments for IUAs. This study aims to confirm the influence of apoptotic bodies of bone marrow mesenchymal stem cells (BMSCs) on endometrial stromal cell fibrosis by mediating the Wnt/β-catenin signaling pathway and to provide new insight for the clinical treatment of IUAs.

Methods: Human endometrial stromal cells (HESCs) were used to establish an IUA cell model by treatment with TGF-β1, and a rat IUA model was established by the double injury method. Apoptosis of BMSCs was detected by TUNEL assays, and cell morphology was observed by the CM-DiI tracer. The morphology of apoptotic vacuoles and apoptotic bodies (ABs) was detected by TEM. We used Western blotting to detect the expression of histone H3.3, histone H2B, C3b, cyclin D1, C1QC, α-SMA, COL1A1, COL5A2, FN, CTGF, Wnt2b, c-MYC, CK-18 and VIM. The expression levels of α-SMA, COL1A1, COL5A2, FN and CTGF were detected by RT−qPCR. The expression levels of α-SMA, COL1A1, FN and CTGF were detected by immunofluorescence. Immunohistochemistry was used to detect the expression of TGF-β, CK-18 and VIM. Flow cytometry, cell scratch assays, CCK-8 assays, and H & E and Masson staining were used to detect the cell cycle, cell migration, cell proliferation, and endometrial pathology, respectively.

Results: We found that ultraviolet light (UV) irradiation induced apoptosis of BMSCs and increased the production of ABs. TGF-β1 treatment can induce HESCs to form extracellular matrix (ECM), and aggravate cell fibrosis, and adding ABs or FH535, an inhibitor of the Wnt/β-catenin signaling pathway, can inhibit TGF-β1-induced HESC fibrosis. However, the inhibitory effect of ABs on TGF-β1-induced fibrosis of HESCs was attenuated by the addition of LiCl. In the Wnt/β-catenin signaling pathway, LiCl is an activator after coculture with TGF-β1. In vivo, IUA-induced narrowing of the uterine cavity was accompanied by intrauterine adhesions, increased deposition of

* Corresponding authors. First Affiliated Hospital of Kunming Medical University, Kunming, Yunnan,650032 , China ; Yan 'an Hospital Affiliated to Kunming Medical University , Kunming, Yunnan, 650051, China.
E-mail address: hanxuesong@kmmu.edu.cn (X. Han).
[1] These authors have contributed equally to this work.

https://doi.org/10.1016/j.heliyon.2023.e20716
Received 7 June 2023; Received in revised form 18 September 2023; Accepted 4 October 2023
Available online 13 October 2023
2405-8440/© 2023 Published by Elsevier Ltd. This is an open access article under the CC BY-NC-ND license (http://creativecommons.org/licenses/by-nc-nd/4.0/).

collagen fibers, upregulation of TGF-β1, VIM, α-SMA, COL1A1 and COL5A2, and downregulation of CK-18. These changes in expression were reversed after treatment with ABs or FH535. When ABs and LiCl were added at the same time, the inhibitory effect of ABs on IUA fibrosis was weakened.

Conclusion: BMSC-derived ABs inhibit the fibrosis of HESCs by inhibiting the Wnt/β-catenin signaling pathway. These results provide a new direction for the clinical treatment of IUAs.

1. Introduction

Intrauterine adhesions (IUAs) are a common disorder of the uterine cavity that produces abnormal adhesions in the uterus and/or cervix caused by mechanical injury or infection [1]. IUAs can lead to the destruction of endometrial tissue structure, abnormal menstruation, periodic pelvic pain, uterine cavity blockage, and even infertility and repeated abortion in severe cases [2]. Endometrial fibrosis is the main pathological feature of IUAs and is characterized by abnormal collagen deposition and endometrial scarring/adhesions, endometrial stromal cell proliferation, increased fibroblasts, and increased extracellular matrix secretion [3]. In addition, studies have shown that patients with severe IUAs are prone to relapse after surgery and are not prone to pregnancy [4]. Nevertheless, there is still no effective treatment for IUA. Therefore, it is important to find new treatments to improve the treatment of IUA..

Bone marrow mesenchymal stem cells (BMSCs) are multipotent stem cells with potent self-replication and differentiation that are widely used in cell therapy and transplantation [5]. BMSCs can generate a series of growth factors and cytokines, which can inhibit inflammation, reduce apoptosis, reverse fibrosis and enhance cell function [6]. BMSCs have the potential to differentiate across systems and lineages. They can differentiate into osteoblasts, chondrocytes, endothelial cells, nerve cells and other mesodermal cells and neuroectodermal cells and have an active role in the repair of tissue injury. BMSCs can migrate and accumulate in the endometrial tissue to repair the damaged endometrium [7]. Moreover, BMSCs can effectively alleviate the progression of IUAs by promoting angiogenesis [8]. Moreover, BMSC-derived exosomes can effectively inhibit endometrial adhesion and fibrosis during endometrial repair [9]. Apoptotic bodies (ABs) are membrane-bound vesicles produced by apoptotic cells during the final phase of apoptosis [10] and contain a variety of functional biomolecules that can diffuse within the tissue, trigger compensatory proliferation of surrounding cells and maintain tissue homeostasis after the wound [11]. The mechanism by which ABs derived from mature osteoclasts promote osteogenic differentiation is through RANKL-mediated reverse signaling [12]. In tissue repair, transplanted MSCs can promote skin wound healing by releasing ABs [13]. However, the therapeutic potential of ABs derived from BMSCs in IUA cases and their mechanisms of action have not been explored.

As a highly conserved and tightly controlled molecular mechanism, the Wnt/β-catenin signaling pathway is involved in various cellular processes in the female genital system and has a key role in decidualization of the endometrium, placenta, and establishment of pregnancy [14]. Endometriosis-related fibrosis in uterine disease could be activated by Wnt/β-catenin signaling [15]. The migration and epithelial-mesenchymal transition (EMT) of endometrial stromal cells treated with TGFβ can be inhibited by related miRNAs by targeting the Wnt/β-catenin pathway [16]. In addition, the Wnt/β-catenin signaling pathway participates in the progression of endometrial stromal cell fibrosis in IUAs [4]. However, there is no research on the inhibition of endometrial stromal cell fibrosis by BMSC-derived ABs mediated by the Wnt/β-catenin signaling pathway. Therefore, we isolated ABs from BMSCs by ultraviolet irradiation and constructed IUA cell and animal models in this study. Cell and animal experiments were carried out to analyze the influence of the AB-mediated Wnt/β-catenin signaling pathway on endometrial stromal cells and its mechanism, hoping to offer new strategies for the clinical treatment of IUAs.

2. Materials and methods

2.1. Culture, treatment and identification of BMSCs

hBMSCs were purchased from ScienCell (San Diego, CA, USA) and cultured in the presence of 10 % fetal bovine serum (Gibco, USA), 100 μM L-ascorbic acid, 2 mM L-glutamine (Gibco), 0.1 U/L penicillin (Gibco), and 0.1 μg/L streptomycin (Gibco) in low glucose DMEM (Gibco). The parameters of the cell incubator were 37 °C and 5 % CO_2, and a microscope was used to observe the morphology of the cells. The culture medium was changed and passaged routinely. Monolayer hBMSCs were stored in a Petri dish and irradiated with 600 mJ/cm^2 intensity UVC light (30 W, 254 nm, Philip, China) for 25 min [11]. The apoptosis of hBMSCs was detected by the TdT-mediated dUTP nick end labeling (TUNEL) method (MA 0224, Meilun Biology, China), and the cell morphology was observed by a CM-DiI live cell tracer (red). Apoptotic vesicles and vacuoles in UV-treated hBMSCs were observed by transmission electron microscopy (Tecnai T10, Philips, Netherlands).

2.2. Isolation and identification of ABs

The UV-treated hBMSCs were further cultured for 24 h, and then, the supernatant was collected by continuous centrifugation [11]. Purified ABs were quantified with a bicinchoninic acid (BCA) protein assay kit. ABs morphology was observed by transmission electron microscopy (Tecnai T10, Philips, Netherlands). The antibodies were characterized by Western blot analysis of the expression of the ABs marker protein. As a control, extracellular vesicles (EV) were isolated from the culture medium of hBMSCs without UV treatment by

Table 1
Primer sequences for RT−qPCR.

Target gene	Forward	Reverse
α-SMA	5′-GCTCCAGTTCCTTGTCCTCC-3′	5′-CTCACGACTTTCACCTTCGGTA-3′
COL1A1	5′-AAGGTGTTGTGCGATGACG-3′	5′-ACAACACGCTACTGCACTAG-3′
COL5A2	5′-TGTGCCGACCCTGTAACGC-3′	5′-TTTACCGACCCAACCTAC-3′
FN	5′-GGAGAATGTCAGCCCACCAA-3′	5′-CAACTACGGCAAGGTCGG-3′
CTGF	5′-AGGGCCTCTTCTGTGACTTCG-3′	5′-GAAGACACTGAAGCCGAGGG-3′
GAPDH	5′-GACCACAGTCCATGCCATCA-3′	5′-GTCGCTGTTGAAGTCAGAGGAG-3′

the same isolation method as the ABs.

2.3. TUNEL staining

Apoptosis was assessed using a TUNEL assay kit (MA 0224, Meilun Biology, China). Briefly, cells were fixed with 4 % paraformaldehyde, and permeabilized with 0.1 % Triton ® X-100. In a wet box at 37 °C, the TUNEL reaction mixture was added and incubated for 60 min. Nuclear staining was performed with DAPI. The results were observed using a fluorescence microscope.

2.4. CM-DiI staining

According to the instructions of the CellTracker CM-DiI living cell tracer (40718ES50, Yeasen, China), the cells were incubated in CM-DiI staining solution at 37 °C for 3 min and then incubated at 4 °C for 15 min for fluorescence labeling. After labeling, the cells were washed with PBS. The cells were fixed with 3.7 % formaldehyde for 10 min, washed twice with PBS at room temperature, permeabilized with acetone at −20 °C for 10 min, and then washed with PBS. The results were observed using a fluorescence microscope.

2.5. Western blot

The tissue and cells were first frozen and ground in liquid nitrogen, and then, RIPA lysis solution was added for lysis. The concentration was detected by a BCA reaction kit. After quantitative analysis, the total protein was denatured in this study. An SDS−PAGE gel was used for electrophoresis, and the electrophoresis apparatus (Bio-Rad, USA) was adjusted to 120 V for electrophoresis. A PVDF membrane (Millipore, USA) was used for membrane transfer, and skim milk (Sigma, USA) was used for blocking. Prediluted primary antibodies were as follows (Abcam, USA): histone H3.3 (1:1000, ab176840, Abcam, USA), histone H2B (1:10000, ab40886, Abcam, USA), C3b (1:100, ab231080, Abcam, USA), C1QC (1:1000, ab75756), α-SMA (1:1000, ab5831), COL1A1 (1:5000, ab138492), COL5A2 (1:1000, ab7046), FN (1:5000, ab45688), CTGF (1:1000, ab209780), Wnt2b (1:1000, ab178418), c-MYC (1:1000, ab32072), Cyclin D1 (1:1000, ab16663), CK-18 (1:20000, AB133263), VIM (1:5000, AB92547) and β-catenin (1:10000, AB32572) were incubated overnight at 4 °C. The next day, goat anti-mouse antibody (1:2000; Abcam, UK) or goat anti-rabbit antibody was added and incubated for 1 h with slow shaking at 25 °C. ECL chemiluminescence solution was used for development, a chemiluminescence instrument was used for exposure and observation, and ImageJ was used for protein band analysis.

2.6. Construction of the IUA cell model

Human endometrial stromal cells (HESCs) were purchased from ATCC (Manassas, USA). After treatment with TGF-β1 (10 ng/mL) for 72 h, the IUA cell model was constructed according to the literature [4]. Cell grouping: Control group: HESC cells were cultured normally for 24 h without any interference. TGF-β1 group (model group): TGF-β1 (10 ng/mL) was used to treat HESCs for 72 h. TGF-β1 + NC group: On the basis of the model group, 24 μg/mL PBS buffer was added for 24 h. TGF-β1 + AB group: On the basis of the model group, 24 μg/mL ABs were added for 24 h. TGF-β1 + FH535 group: On the basis of the model group, 20 μM of the Wnt/β-catenin signaling pathway inhibitor FH535 was added for 24 h. TGF-β1 + ABs + LiCl group: On the basis of the model group, ABs and 10 mM of the Wnt/β-catenin signaling pathway activator LiCl were added for 24 h.

2.7. RT−qPCR

An RNA kit was used to obtain total RNA. Care was taken to avoid RNA degradation and contamination during extraction. The cells were frozen in liquid nitrogen, and then, TRIzol reagent was added to isolate total RNA. Fluorescence quantitative PCR was performed using cDNA with the extent of reaction: predenaturation at 95 °C for 20 s. Then, the amplification cycle was carried out at 95 °C for 1 s and 60 °C for 20 s, and there were 40 cycles in this stage. Then, a dissolution curve analysis stage was performed, wherein the temperature of the dissolution curve was set to 60–95 °C, and each sample was provided with three duplicate wells. With β-actin as a control, the level of the target product relative to the internal control was expressed as $2^{-\Delta\Delta Ct}$. The primer sequences were as follows (see Table 1):

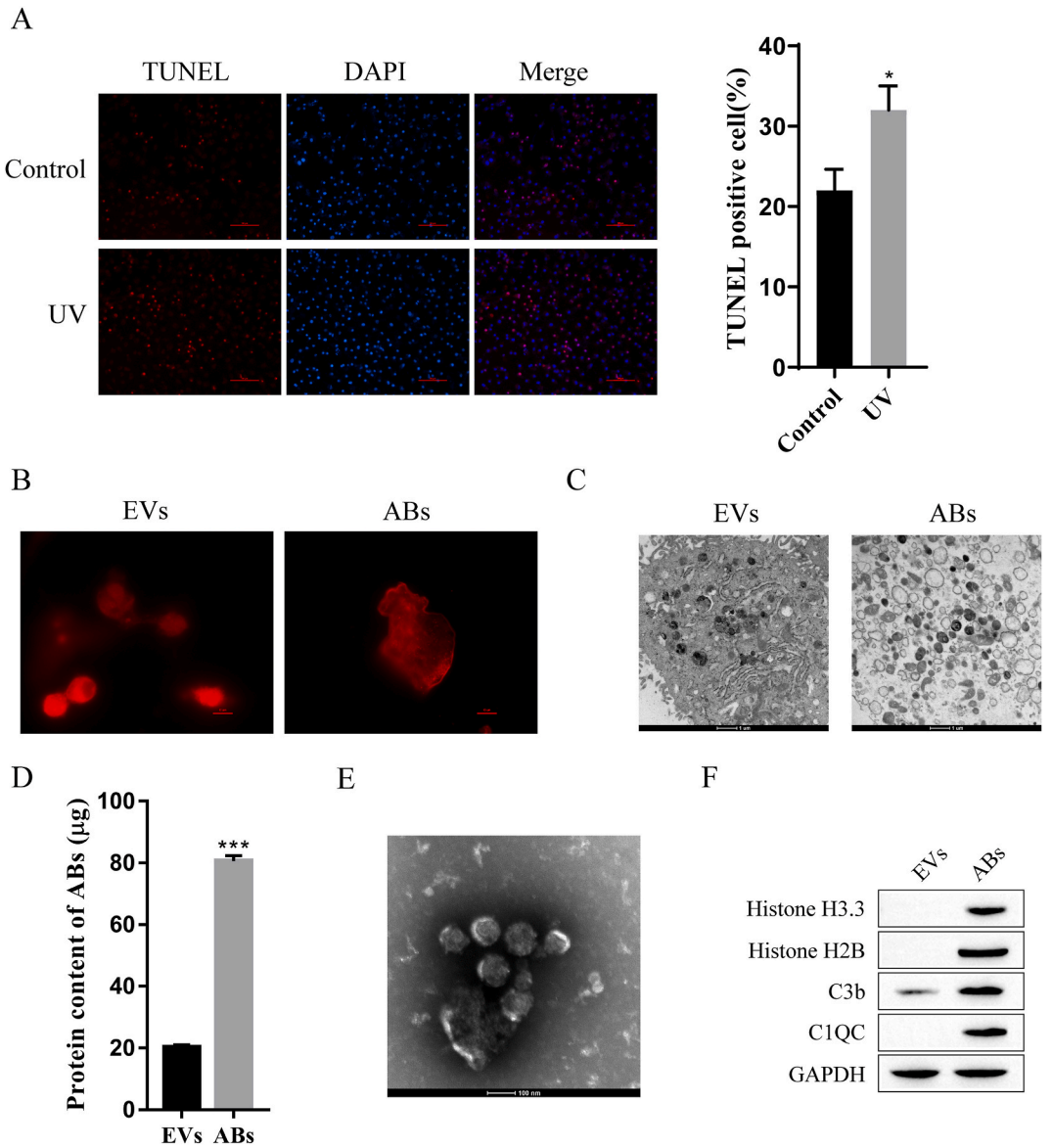

Fig. 1. Identification of apoptotic bodies derived from BMSCs (A) TUNEL was used to detect the apoptosis level of BMSCs (scale = 100 μm); (B) CM-DiI was used to observe the cell morphology (scale = 10 μm); (C) Transmission electron microscopy was used to observe the changes of apoptotic vesicles and vacuoles; (D) Purify ABs by continuous centrifugation, and performing quantitative analysis on that concentration of ABs by use a BCA protein detection kit after purification; (E) Observing the morphology of ABs through a transmission electron microscope; (F) Detecting the expression of the ABs mark protein by Western Blot. ***P < 0.001 vs Control or EVs. EVs, group of outer vesicles of UV-untreated BMSCs. ABs, group of apoptotic vesicles of UV-treated BMSCs. Each experiment was repeated three times.

2.8. Immunofluorescence

Cells were grown on glass covers overnight to prepare cell slides, which were then fixed with 4 % paraformaldehyde. Then, Triton X-100 (0.2 %) was used to permeabilize the cells, and 1 % bovine serum albumin was used to block the cells. Then, at 4 °C, the cells were cultured with primary antibodies against α-SMA (1:250, ab108531, Abcam, USA), COL1A1 (1:500, ab36064, Abcam, USA), FN (1:50, ab268020, Abcam), and CTGF (1:50, Ab 268020, Abcam, USA) for 12 h. After that, we used PBS to wash the samples and then incubated them with fluorescently labeled secondary antibodies (1:1000, ab150077, Abcam, USA) for 1 h in the dark. Finally, DAPI (Invitrogen, CA, USA) was added for counterstaining, and the results were observed and imaged using a fluorescence microscope.

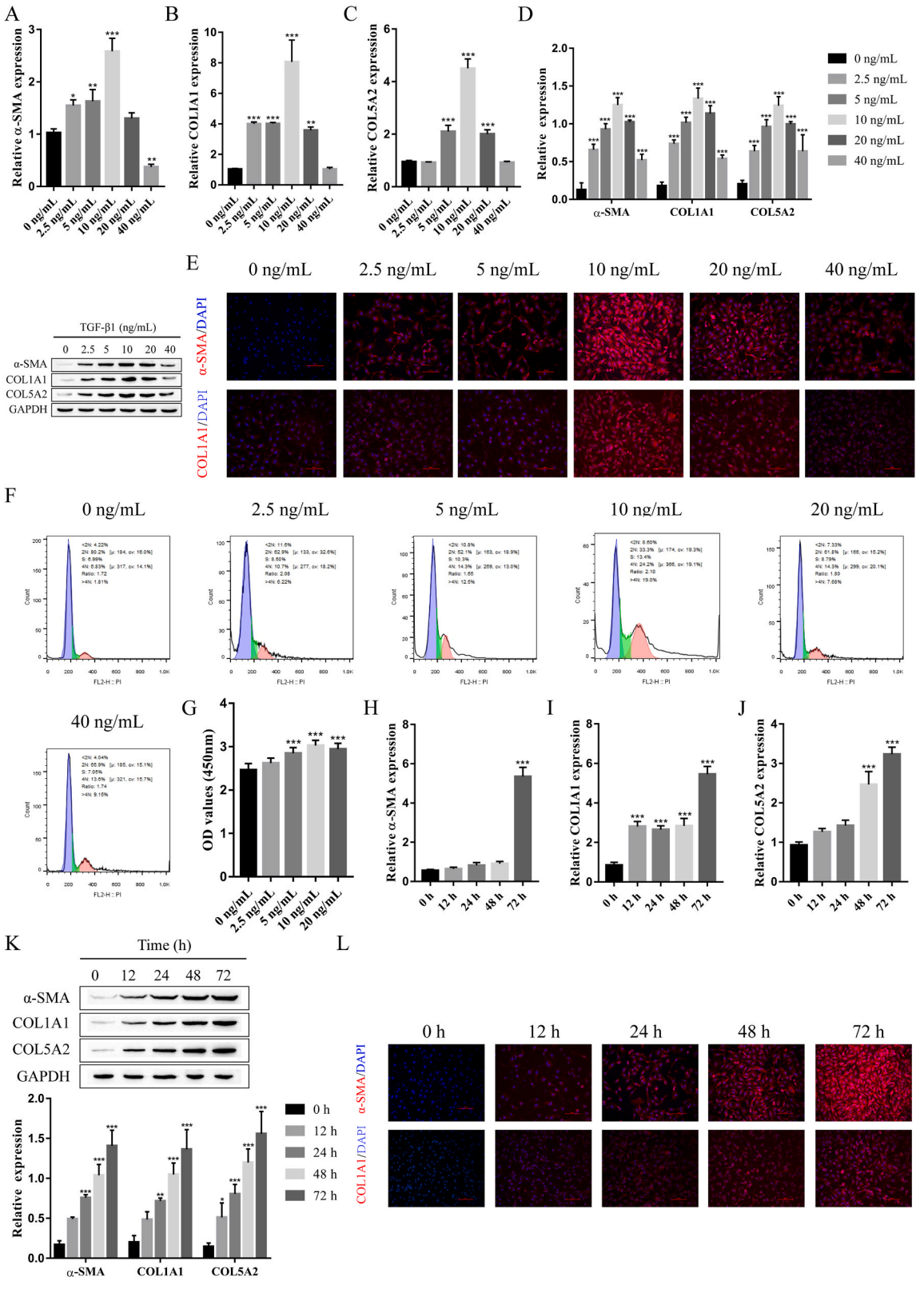

(caption on next page)

Fig. 2. Fibrosis of primary HESCs induced by TGF-β1 (A) RT−qPCR was used to detect the mRNA level of α-SMA; (B) RT−qPCR was used to detect the mRNA level of COL1A1; (C) RT−qPCR was used to detect the mRNA level of COL5A2; (D) Western blotting was used to detect the protein level of fibrosis-related proteins; (E) Immunofluorescence was used for the expression of fibrosis-related proteins (scale bar = 100 μm); (F) The cell cycle was assessed by flow cytometry; (G) Cell proliferation was assessed by CCK-8 assays; (H) Expression of α-SMA was determined by RT−qPCR; (I) Expression of COL1A1 was determined by RT−qPCR; (J) COL5A2 expression was determined by RT−qPCR; (K) Fibrosis-related protein expression was determined by Western blotting; (L) Fibrosis-related protein expression was determined by immunofluorescence (scale bar = 100 μm). *P < 0.05, **P < 0.01, ***P < 0.001 vs 0 ng/mL or 0 h. Each experiment was repeated three times.

2.9. Flow cytometry

In this study, we used flow cytometry to detect the cell cycle. First, 70 % ethanol was precooled, and the cells were incubated. Then, the cells were collected by centrifugation. After that, PBS was used to resuspend the cells twice, and RNase A (50 μg/mL) was used to incubate the cells for 20 min. Then, 50 μg/mL propidium iodide (PI) was used to incubate the cells for 30 min in the dark. Finally, flow cytometry (Verse, BD, USA) was used for detection.

2.10. CCK-8 assays

The CCK-8 kit (Solarbio, Beijing) was used in this study. HESC cells were cultured in an incubator environment (37 °C, 5 % CO_2) for preculture in 96-well plates. After transfection or dosing, 10 μL of CCK-8 reagent was added, and the cells were cultured for 2 h. Finally, an enzyme marker (ELX800, BioTeK, UK) was used to measure the absorbance at 450 nm.

2.11. Cell scratch assay

In 6-well plates, 1×10^5 cells were inoculated, and the cells were scratched with a pipette tip and washed three times. The scratched cells were removed, and the residual cells were cultured in an incubator environment (37 °C, 5 % CO_2). A microscope was used to take pictures for analysis.

2.12. Construction of the IUA animal model

All animal experiments in this study were approved by the Animal Experiment Ethics Review Committee of Kunming Medical University (Approval number: kmmu20220879), and all methods conformed to the stipulations of the National Institutes of Health Office of Laboratory Animal Welfare policies and laws.

Sixty 9-week-old female Sprague−Dawley rats (230 ± 20 g) were purchased from the Animal Experimental Center of Kunming Medical University (Kunming, China). For the rats, food and water were plentiful. The rats were given food and water ad libitum, and there were 4–5 rats in each cage with a 12-h light/dark cycle. Rat IUA model was established of right uterus by double injury method [17]. There were 6 groups, and the rats were randomly divided. In the control group, the rats were fed routinely. In the IUA group, IUA was induced in rats without any intervention or treatment. In the IUA + NC group, the rats were induced by IUA, and after 2 weeks, the abdomen was opened again, and normal saline (0.2 mL) was injected into the right corner of the uterus. Then, normal saline was injected intraperitoneally 3 consecutive times once every 5 days. For the IUA + AB group, rats were induced by IUA, and then, the abdomen was opened again after 2 weeks. ABs (96 μg/kg, suspended in saline) were injected into the right corner of the uterus, and then, ABs were injected intraperitoneally 3 consecutive times once every 5 days. For the IUA + FH535 group, rats were induced by IUA, injected with 7 mg/kg FH535 intraperitoneally after 2 weeks, and then injected with FH535 intraperitoneally 3 consecutive times once every 5 days. For the IUA + AB + LiCl group, the rats were induced by IUA, and then, the abdomen was opened again after 2 weeks. ABs and 0.1 mg/kg LiCL were injected into the right corner of the uterus, and then, ABs and LiCL were injected intraperitoneally 3 consecutive times once every 5 days.

2.13. Hematoxylin-eosin (H & E) and Masson staining

For H & E and Masson staining, we used 4 % paraformaldehyde to fix the endometrial tissue cells for 12 h and dehydrated them with an ethanol gradient. Then, we used paraffin to embed the tissue. H & E and Masson trichrome staining were used to stain sections (5 μm). The results were observed using a fluorescence microscope.

2.14. Immunohistochemistry

Rat endometrial tissue was washed with PBS, and paraffin sections were prepared. The sections were subjected to routine dewaxing Subsequently, the tissue sections were incubated with freshly preheated antigen extraction buffer and equilibrated at room temperature for 30 min. After washing with PBS, the sections were incubated with the following primary antibodies (Abcam, USA) overnight at 4 °C: TGF-β1 (1:500, ab215715), CK-18 (1:500, ab133263), and VIM (1:250, ab92547). The primary antibody was discarded the next day, and after three PBS washes, the tissue was treated with secondary antibody (1:500, ab97051) for 30 min at room temperature. Finally, DAB coloration and hematoxylin counterstaining were performed. Then, DAB was used to stain the sections, and they were dehydrated and sealed for observation and analysis.

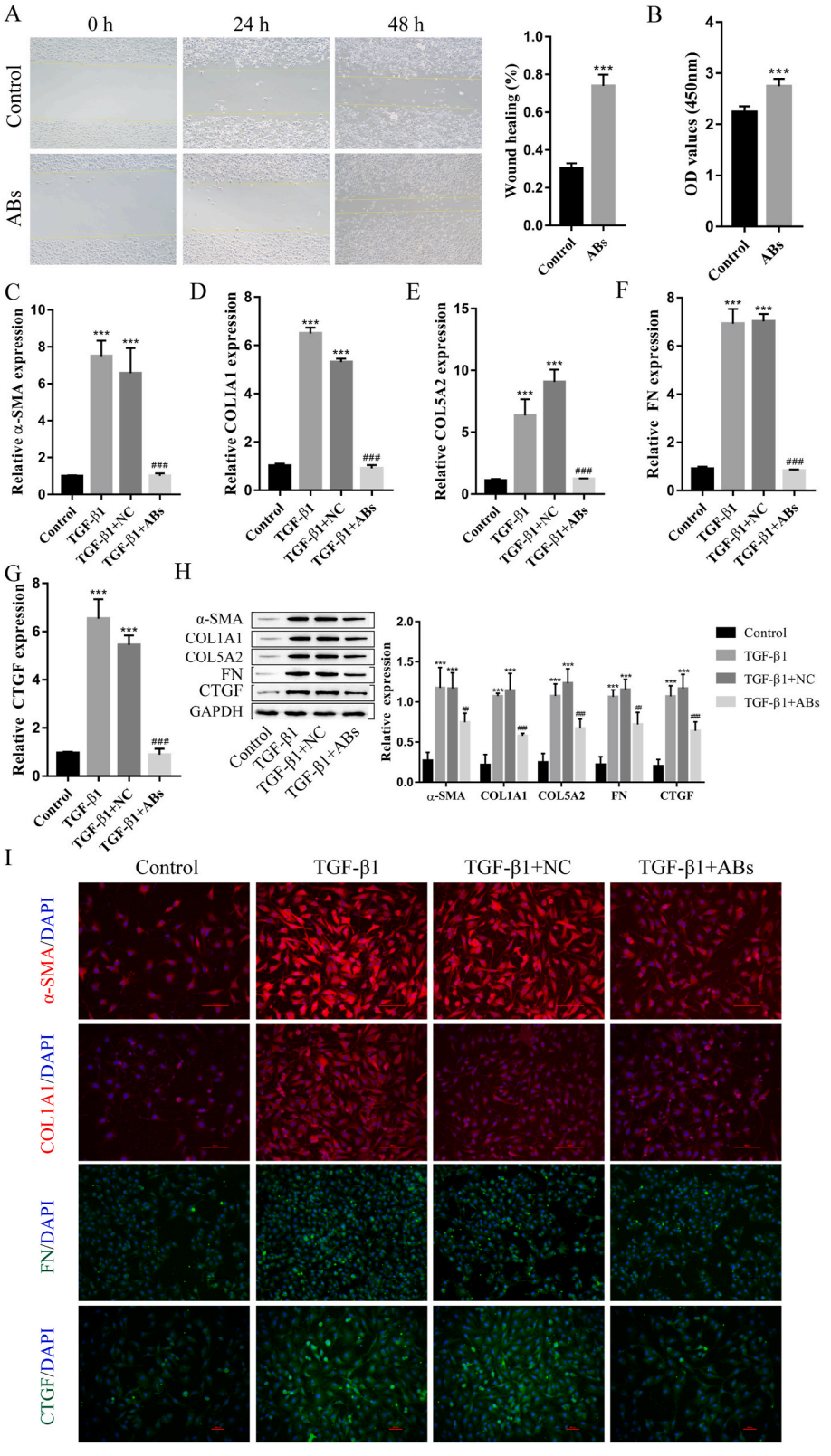

(caption on next page)

Fig. 3. BMSC-derived apoptotic bodies inhibit TGF-β1-induced fibrosis in HESCs (A) The migration of HESCs was detected by cell scratch test; (B) CCK-8 assays were used to detect the proliferative ability; (C) RT−qPCR was used to detect the mRNA level of α-SMA; (D) RT−qPCR was used to detect the mRNA level of COL1A1; (E) RT−qPCR was used to detect the mRNA level of COL5A2; (F) RT−qPCR was used to detect the mRNA level of FN; (G) RT−qPCR to detect the mRNA level of CTGF; (H) Western blot was used to detect the protein level of fibrosis-related proteins; (I) Immunofluorescence was used to detect the protein level of fibrosis-related proteins (scale bar= 100 μm). ***P < 0.001 vs Control;$^{\#\#}$P < 0.01,$^{\#\#\#}$P < 0.001 vs TGF-β1+NC. Each experiment was repeated three times.

2.15. Data statistics

For all statistical analyses, statistical analyses GraphPad Prism7 was used. All experiments were divided into three parallel groups, and the experiment was repeated three times at least. Results are presented as mean and SD value. Two-way ANOVA was used for the multi-group comparison, and *t*-test was used for the between-group comparison. $P < 0.05$ difference was statistically significant.

3. Results

3.1. Identification of BMSC-derived Apoptosomes

The TUNEL results showed that the apoptosis of BMSCs treated with ultraviolet (UV) light was significantly higher than that of BMSCs without UV treatment (Fig. 1A). After CM-DiI labeling, the expression of fluorescence in BMSCs without UV treatment was stable, the positive labeling rate was more than 98 %, and the cell morphology was good, while after CM-DiI labeling, the expression of fluorescence in BMSCs with UV treatment was weakened, and the cell morphology was irregular (Fig. 1B). The transmission electron microscopy results showed that apoptotic vesicles and vacuoles were altered in the UV-treated cells (Fig. 1C). After purification by centrifugation, the protein content of ABs in the UV-treated cells was significantly higher than that of extracellular vesicles (EVs), indicating that UV treatment increased the production of ABs (Fig. 1D). ABs were observed to be spherical under transmission electron microscopy (Fig. 1 E), and specific markers of ABs, such as histone H3.3, histone H2B, C3b, and C1QC, could be expressed (Fig. 1F). In conclusion, UV irradiation induced apoptosis of BMSCs, decreased the expression of CM-DiI fluorescence, changed the morphology of apoptotic vesicles and vacuoles, and increased the production of ABs. ABs were spherical in shape, and the expression of histone H3.3, histone H2B, C3b and C1QC was upregulated during the production of ABs.

3.2. TGF-β1 induces fibrosis in primary human endometrial stromal cells (HESCs)

TGF-β1 induced the upregulation of α-SMA, COL1A1, and COL5A2 in HESCs in a concentration-dependent manner, as shown by RT−qPCR and Western blot assays (Fig. 2A–D), with 10 ng/mL as the cutoff value. Immunofluorescence results showed (Fig. 2E) that α-SMA and COL1A1 could be upregulated by TGF-β1 in HESCs in a concentration-dependent manner, with a cutoff level of 10 ng/mL. With the increase in TGF-β1 concentration, there was a decreased ratio of G0/G1 (2 N) phase cells, while there was an increased ratio of S phase cells. When TGF-β1 was greater than 10 ng/mL, the above trend was reversed (Fig. 2F). The CCK-8 results showed that the proportion of proliferating cells increased gradually at first and then decreased (Fig. 2G). Further experimental results showed that the upregulation of α-SMA, COL1A1 and COL5A2 in HESCs could be induced by TGF-β1 in a time-dependent manner (Fig. 2H–K), and 72 h was the optimal TGF-β1 treatment time. Through immunofluorescence experiments, we found that TGF-β1 induced the upregulation of α-SMA and COL1A1 expression in HESCs (Fig. 2L). These data indicate that TGF-β1 can induce fibrosis of HESCs and promote cell proliferation, and TGF-β1 (10 ng/mL) treatment for 3 days was used as the TGF-β1 treatment protocol for subsequent experiments.

3.3. BMSC-derived Apoptosomes inhibit TGF-β1-induced fibrosis in HESCs

In studies of liver fibrosis, BMSC treatment was found to improve liver fibrosis in CCl4-induced fibrotic rats by reducing the expression of fibrosis-related genes and inhibiting collagen deposition in the liver [18]. There is growing evidence that extracellular vesicles (EVs) play a role in the pathogenesis of fibrotic disease [19]. Among them, apoptotic bodies are produced when apoptotic cells contract and die, and extracellular apoptotic bodies are released when cells are activated or apoptosis occurs under inflammatory conditions [20]. In the above experiments, we proved that apoptosis of BMSCs leads to the production of apoptotic bodies. Below, we will further verify whether BMSC-derived apoptotic bodies have an effect on TGF-β1-induced HESC fibrosis. Compared with the controls, the results of the cell scratch assay showed that the healing rate of the ABs group was higher (Fig. 3A), and the proliferation of HESCs in the ABs group was enhanced (Fig. 3B). RT−qPCR showed that TGF-β1 increased the mRNA levels of α-SMA, COL1A1, COL5A2, FN and CTGF compared with those of the control group, and the addition of ABs effectively reversed the expression of these fibrosis-related proteins (Fig. 3C–G). The Western blot results showed that TGF-β1 induced upregulation of fibrosis-related protein expression, and fibrosis-related proteins in the TGF-β1+ABs group were significantly lower than those in the TGF-β1+NC group (Fig. 3H). Moreover, TGF-β1 induction increased the positive expression of α-SMA, COL1A1, FN and CTGF in HESCs, while the expression was reversed after coculture with ABs (Fig. 3I). These results indicate that BMSC-derived ABs can inhibit the induction of fibrosis in HESCs by TGF-β1.

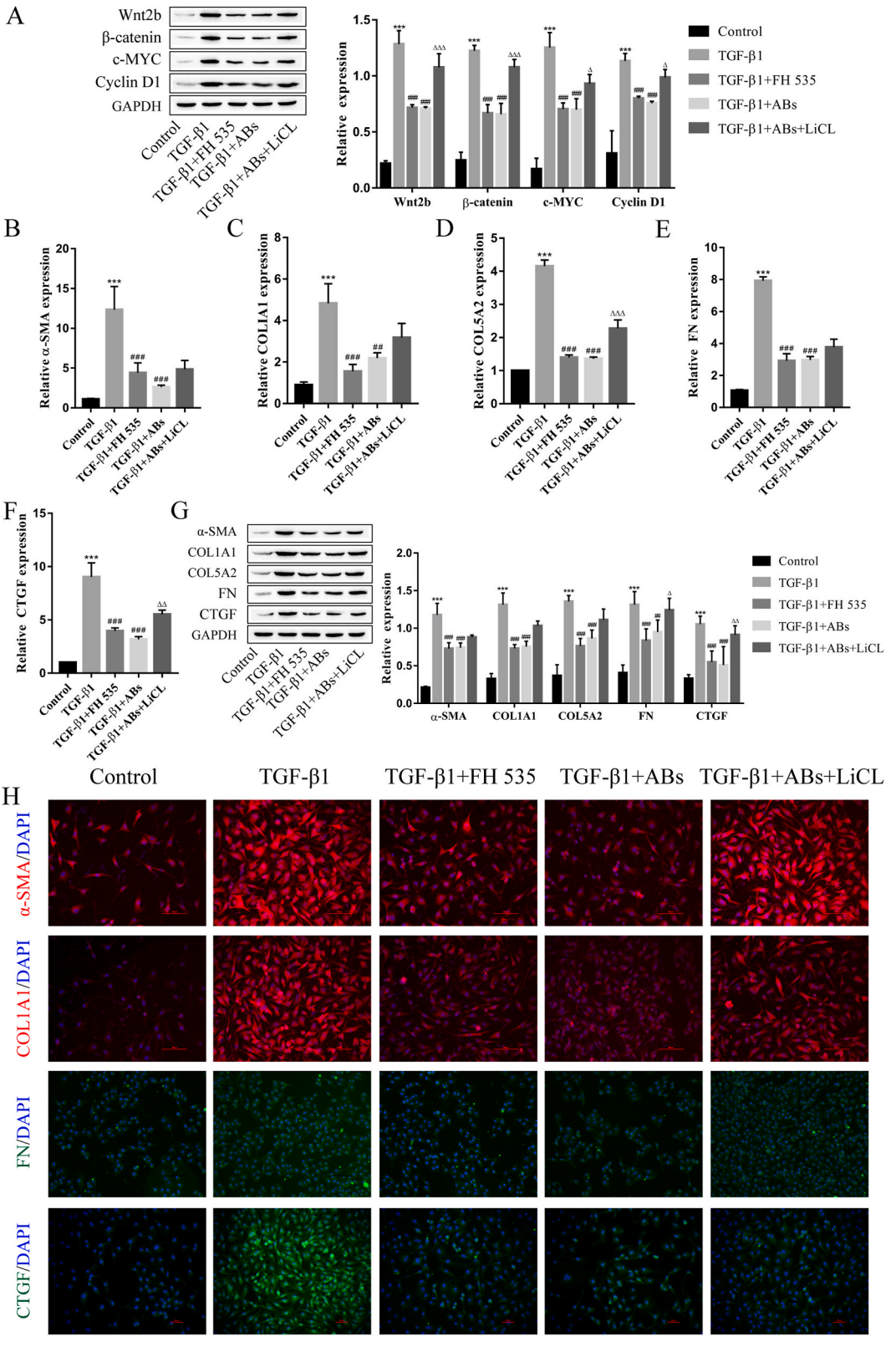

(caption on next page)

Fig. 4. BMSC-derived apoptotic bodies inhibit TGF-β1-induced fibrosis of HESCs by mediating the Wnt/β-catenin signaling pathway (A) Western blots were used to detect the protein level of Wnt/β-catenin signaling pathway-related proteins; (B) RT−qPCR was used to detect the mRNA level of α-SMA; (C) RT−qPCR was used to detect the mRNA level of COL1A1; (D) RT−qPCR was used to detect the mRNA level of COL5A2; (E) RT−qPCR was used to detect the mRNA level of FN; (F) RT−qPCR was used to detect the mRNA level of CTGF; (G) Western blots were used to detect the protein level of fibrosis-related protein; (H) Immunofluorescence was used to detect the protein level of fibrosis-related protein (scale bar = 100 μm). ****P < 0.001 vs Control;$^{\#\#}$P < 0.01,$^{\#\#\#}$P < 0.001 vs TGF-β1;$^{\triangle}$P < 0.05,$^{\triangle\triangle}$P < 0.01,$^{\triangle\triangle\triangle}$P < 0.001 vs TGF-β1+ABs. Each experiment was repeated three times.

3.4. BMSC-derived Apoptosomes inhibit TGF-β1-induced fibrosis of HESCs by mediating the Wnt/β-catenin signaling pathway

Compared with those in the control group, the levels of the Wnt/β-catenin signaling pathway-related proteins Wnt2b, β-catenin, c-MYC and cyclin D1 were increased in the TGF-β1 group, as shown by Western blot assays. However, the expression was reversed by adding FH535, which could be an inhibitor of the Wnt/β-catenin signaling pathway, or coculture with ABs. Furthermore, after coculture with TGF-β1, LiCl, an activator of the Wnt/β-catenin signaling pathway, was added. The inhibitory effect of ABs on TGF-β1-induced fibrosis of HESCs was attenuated (Fig. 4A). TGF-β1 induced the expression upregulation of α-SMA, COL1A1, COL5A2, FN and CTGF. However, the effect of TGF-β1 on HESC fibrosis was reduced by adding FH535 or coculturing with ABs, and adding LiCl attenuated the inhibitory effect of ABs on TGF-β1-induced fibrosis of HESCs (Fig. 4B–G). Finally, similar results were obtained by further verification of the immunofluorescence experiments (Fig. 4H). These results suggest that BMSC-derived ABs inhibit the induction of fibrosis in HESCs by TGF-β1 through inhibition of the Wnt/β-catenin signaling pathway.

3.5. BMSC-derived apoptotic bodies inhibit endometrial fibrosis in rats

We confirmed the inhibition of TGF-β1 by BMSCs cell-derived ABs on the induction of HESCs fibrosis by in vitro experiments, and we will further verify the effect of BMSCs cell-derived apoptotic bodies on endometrial fibrosis in rats. H & E staining showed that the endometrium was intact and the glands were evenly distributed in the Control group, whereas the endometrial layer of the uterine tissues of the rats in the IUA group was disrupted, with a large number of inflammatory cells infiltrating and the number of glands was significantly reduced, whereas treatment with ABs resulted in a thickening of the endometrium, an increase in the number of glands and a decrease in the inflammatory cell infiltration (Fig. 5A). In the endometrial stroma of the control group, there was no collagen fiber deposition. However, the deposition of collagen fibers was significantly increased in the IUA group and IUA + NC group. However, the deposition of collagen fibers in the endometrium of the IUA + ABs group was significantly reduced compared with that of the IUA + NC group (Fig. 5B). CK-18 is a cytoskeletal protein that mainly exists in endometrial epithelial cells (EECs) and maintains the integrity of endometrial cells. Its expression decreases after tissue injury. Endometrial stromal cells mainly express vimentin (VIM), and its expression is increased after tissue injury, as well as that of the profibrotic mediator TGF-β1, and positive staining is brown on the cell membrane. Through immunohistochemistry, we found that the level of TGF-β1 in the endometrium of the control group was very low, the expression of CK-18 protein was positive, and the expression of VIM was less. The level of TGF-β1 in the IUA group and IUA + NC group was significantly higher, the positive staining of CK-18 was decreased, and the positive expression of VIM was increased compared with that in the control group. Compared with the IUA + NC group, the IUA + ABs group showed decreased TGF-β1 immunoreactivity, increased CK-18-positive staining, and decreased VIM-positive expression (Fig. 5C). Moreover, the protein levels of α-SMA, COL1A1 and COL5A2 were increased in the IUA group and IUA + NC group compared with the control group, while the levels of α-SMA, COL1A1 and COL5A2 were decreased in the IUA + ABs group compared with the IUA + NC group (Fig. 5D). In summary, BMSC-derived ABs inhibit endometrial fibrosis in rats, and these results further confirm that ABs can alleviate endometrial fibrosis.

3.6. BMSC-derived Apoptosomes inhibit endometrial fibrosis in rats by mediating the Wnt/β-catenin signaling pathway

H&E staining showed that the endometrial layer of the uterine tissue in the IUA group was damaged with a large infiltration of inflammatory cells and a significant reduction in the number of glands as compared to the Control group. Tissue damage was recovered after treatment with the addition of FH 535 or ABs, while LiCl attenuated the therapeutic effect of ABs after treatment with both ABs and LiC1 (Fig. 6A). In the endometrial stroma in the control group, there was almost no collagen deposition in the Masson staining assay. After IUA treatment, there was an increased deposition level of collagen fibers in rat tissues, and the deposition level in the endometrium was significantly reduced in the IUA + FH535 group and IUA + ABs group compared with the IUA group. However, after the simultaneous addition of ABs and LiCl treatment, the deposition was significantly increased compared with that of the IUA + ABs group (Fig. 6B). The immunohistochemistry results showed that the levels of TGF-β1 and VIM in the endometrium of the control group were lower than those of CK-18, while the expression of TGF-β1 and VIM in the endometrium of the IUA group was significantly higher, and the level of CK-18 was decreased. Compared with that of the IUA group, the expression of TGF-β1 and VIM decreased and the expression of CK-18 increased in the IUA + FH535 group and IUA + ABs group. However, the expression of TGF-β1, VIM, and CK-18

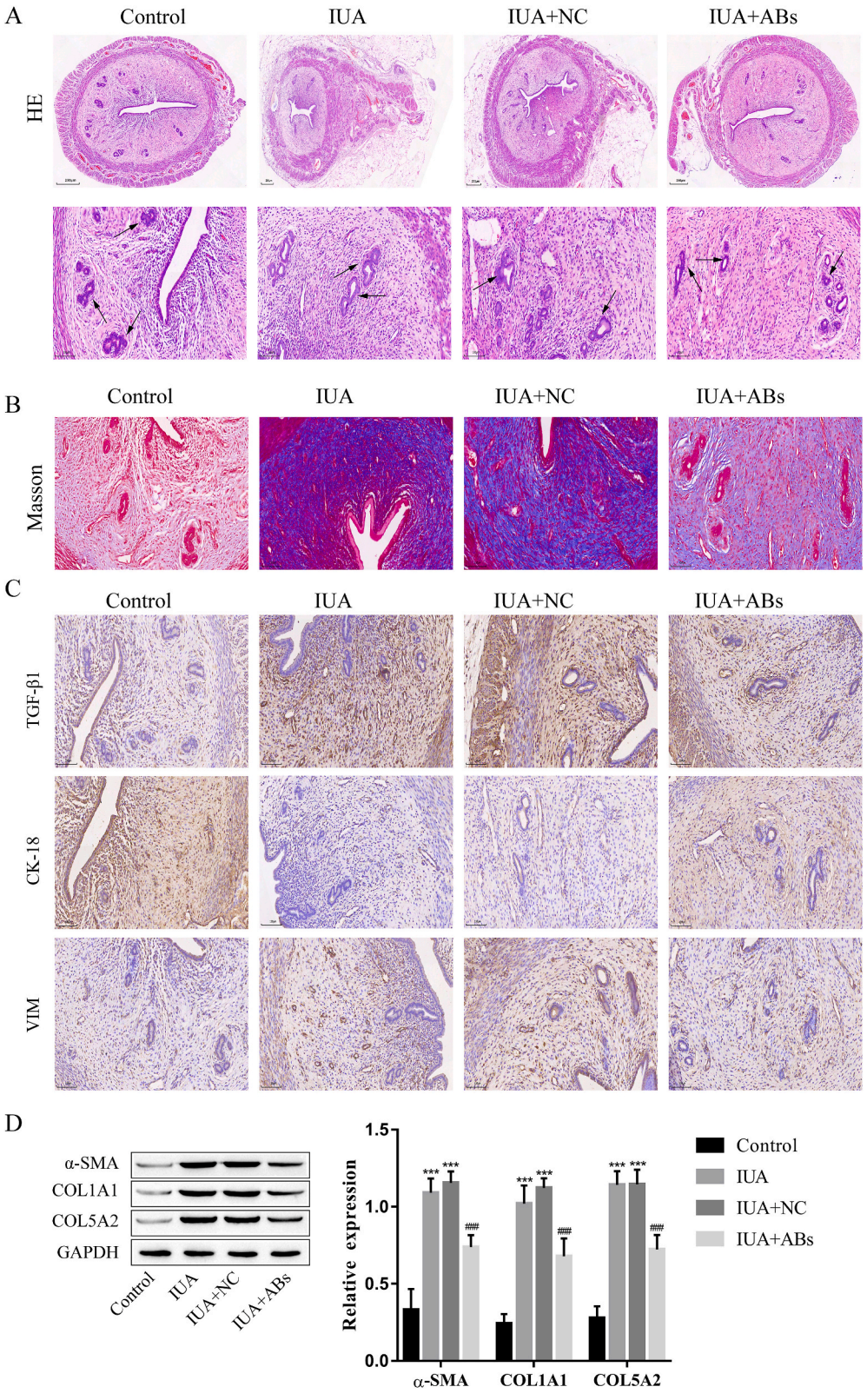

(caption on next page)

Fig. 5. BMSC-derived apoptotic bodies inhibit endometrial fibrosis in rats (A) Pathological changes in uterine sections were observed by H&E staining (scale bar= 100 μm). (B) The degree of endometrial fibrosis was evaluated by Masson staining (scale bar= 100 μm). (C) Immunohistochemistry was used to measure the levels of the TGF-β1, CK-18 and VIM proteins (scale bar= 100 μm). (D) Western blotting was used to measure the levels of fibrosis-related proteins. ***P < 0.001 vs Control; ###P < 0.001 vs IUA + NC. Each experiment was repeated five times.

was reversed by the simultaneous addition of ABs and LiCl treatment (Fig. 6C). Fibrosis-related proteins and Wnt/β-catenin signaling pathway-related proteins were upregulated after IUA treatment. Compared with that of the IUA group, the expression of fibrosis-related proteins was downregulated after FH535 or ABs treatment. Fibrogenic protein expression was increased after the simultaneous addition of ABs and LiCl compared to that in the IUA + ABs group (Fig. 6D–E). In summary, BMSC-derived ABs inhibit rat endometrial fibrosis by inhibiting the Wnt/β-catenin signaling pathway.

4. Discussion

Endometrial fibrosis, as a prominent feature of IUAs, may lead to infertility and recurrent miscarriage. At present, there is no ideal treatment for IUAs. As a member of the TGF-β superfamily, TGF-β1 is essential for the development and maturation of immune cells, the maintenance of immune tolerance and homeostasis, and the regulation of various aspects of the immune response in adult organisms [21]. Increased expression of TGF-β1 has been associated with the progression of renal fibrosis from diabetes, hypertension, obstructive, ischemic, and toxin-induced injury [22]. TGF-β1 also affects pulmonary fibrosis [23], liver fibrosis [24], chondrocyte fibrosis [25] and other fibrotic diseases. Studies have shown that the expression of TGF-β1 is upregulated in IUA progression [26] and is an important mediator of profibrotic stages. Activation of the TGF-β1/Smad pathway promotes endometrial fibrosis [27]. TGF-β1 induction promotes the proliferation and migration of HESCs and enhances the secretion of inflammatory cytokines in vitro [28]. In this study, TGF-β1 induced upregulation of fibrosis-related proteins in HESCs in a concentration- and time-dependent manner in vitro. In vivo, TGF-β1 expression was upregulated after IUA treatment.

The most important pathological feature of IUAs is intrauterine fibrosis. α-SMA, COL1A1, COL5A2, FN and CTGF are specific markers of fibrogenesis and are closely associated with cellular fibrosis [29,30]. In the current study, the expression of these markers was significantly reduced in the BMSC-treated group, suggesting that BMSCs inhibit fibrotic progression and contribute to endometrial epithelial repair [31]. However, the rate of colonization and differentiation of MSCs in host tissues is very low [32]. In recent years, extracellular vesicles (EVs), including exosomes, microvesicles, and ABs, have been found to play an important role in intercellular communication and the regulation of signaling [33]. Yao [34] et al., in a study of damaged endometrium, found that exosomes originating from BMSCs promoted the repair of damaged endometrium. This finding is similar to our study, in which we found that UV irradiation of BMSCs increased the production of ABs, in vitro BMSC-derived ABs inhibited TGF-β1-induced fibrosis of HESCs, and in vivo ABs treatment resulted in the downregulation of TGF-β1 expression and an increase in the number of endometrial glands in rats. These results suggested that BMSCs play biological roles in repairing damaged tissues through ABs, which suggests the potential use of ABs for the treatment of IUA.

A study found that MSCs maintain their stem cell properties by phagocytosing ABs and utilizing multiple cytokines derived from ABs [35]. In addition, researchers have found that MSCs are able to phagocytose ABs via integrin αvβ3 and then inhibit Axin1 using the AB-derived ubiquitin ligases cyclin 146 and miRNA-328-3p to activate the Wnt/β-catenin pathway [36]. Activation of the Wnt/β-catenin signaling pathway has been associated with renal fibrosis [37], pulmonary fibrosis [38], and endometrial fibrosis [39]. During fibrosis, the Wnt/β-catenin signaling pathway works in a combinatorial manner with TGF-β signaling, which induces the expression of Wnt/β-catenin superfamily members [40]. The Wnt/β-catenin signaling pathway plays an important mediating role in the progression of IUAs. For example, si-SNHG5-FOXF2 inhibited TGF-β1-induced fibrosis in human primary endometrial stromal cells through the Wnt/β-catenin signaling pathway [4]. miR-543 inhibited migration and EMT in TGF-β1-treated endometrial stromal cells through both the MAPK and Wnt/β-catenin signaling pathways [16]. In this study, we mainly investigated the mechanism by which ABs affect endometrial fibrosis via Wnt/β-catenin. The addition of FH535, an inhibitor of the Wnt/β-catenin signaling pathway, inhibited the induction of fibrosis in HESCs by TGF-β1, and the addition of the Wnt/β-catenin signaling pathway activator after the coculture of TGF-β1 and ABs with LiCl attenuated the inhibitory effect of ABs on TGF-β1-induced fibrosis in HESCs. However, the molecular mechanism of how ABs regulate the Wnt/β-catenin pathway has not been investigated by us. Most current studies have reported that ABs activate the Wnt/β-catenin pathway by targeting the degradation of Axin via the E3 ubiquitin ligase RNF146 [36], and we will next explore the molecular mechanisms by which ABs regulate the Wnt/β-catenin pathway to provide a theoretical basis for the mechanism of action of ABs in organisms.

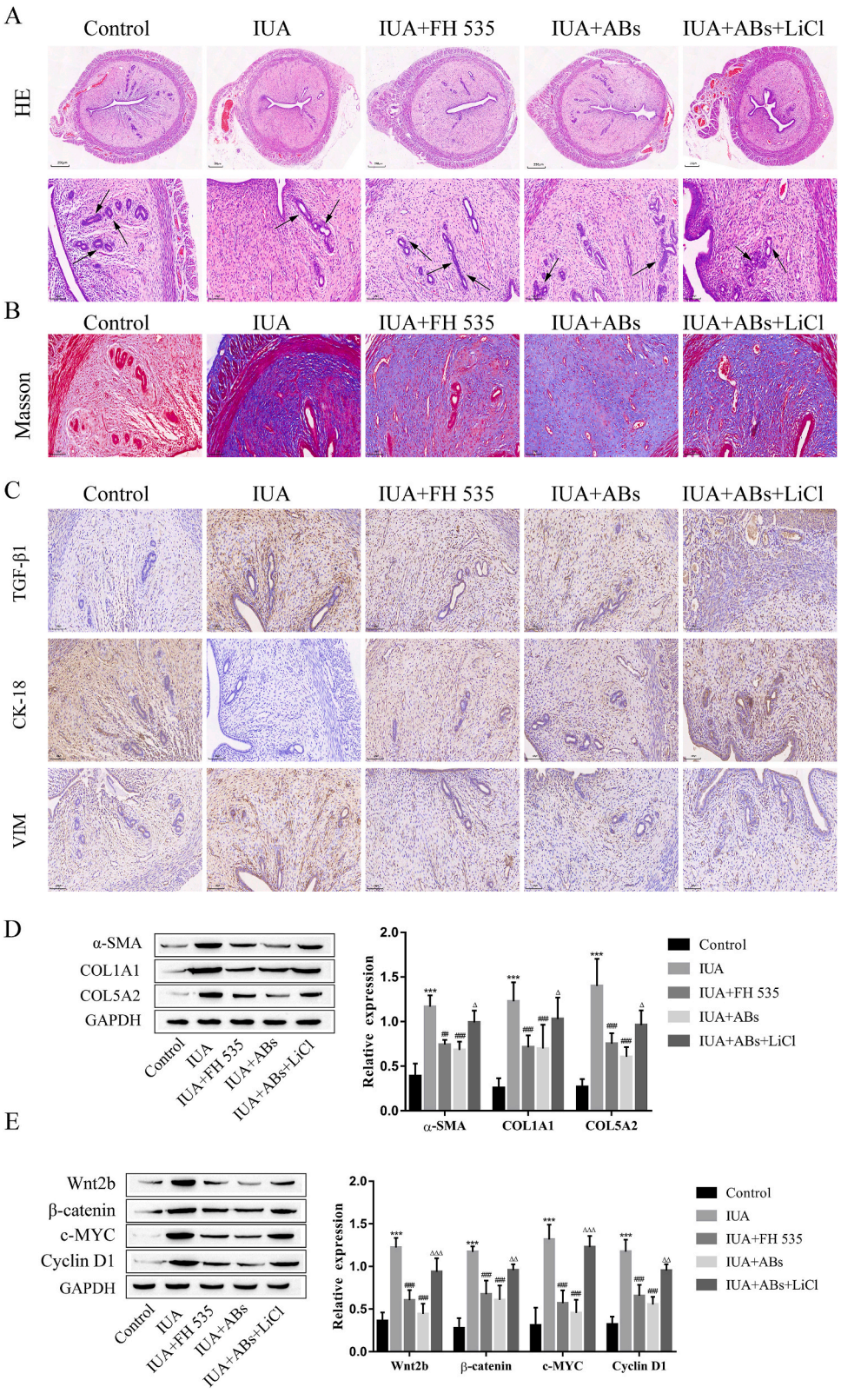

(caption on next page)

Fig. 6. BMSC-derived apoptotic bodies inhibit endometrial fibrosis in rats by mediating the Wnt/β-catenin signaling pathway (A) The pathological changes in uterine sections were determined by H & E staining (scale bar= 100 μm); (B) The degree of endometrial fibrosis was determined by Masson staining (scale bar= 100 μm); (C) The expression of TGF-β1, CK-18 and VIM was determined by immunohistochemistry (scale bar= 100 μm). (D) The levels of fibrosis-related proteins were detected by Western blotting. (E) The levels of Wnt/β-catenin signaling pathway-related proteins were detected by Western blotting. $^{***}P < 0.001$ vs Control; $^{\#\#}P < 0.01$, $^{\#\#\#}P < 0.001$ vs IUA; $^{\triangle}P < 0.05$, $^{\triangle\triangle}P < 0.01$, $^{\triangle\triangle\triangle}P < 0.001$ vs IUA + ABs. Each experiment was repeated five times.

5. Conclusion

In this study, our experimental results demonstrate that BMSC-derived ABs inhibit TGF-β1-induced endometrial stromal cell fibrosis by inhibiting the Wnt/β-catenin signaling pathway, which provides a new idea for the clinical treatment of IUAs.

Ethics approval

The study was approved by the Animal Ethics Committee of Kunming Medical University (Approval number: kmmu20220879) and all methods conformed to the stipulations of the National Institutes of Health Office of Laboratory Animal Welfare policies and laws.

Author contribution statement

Zhenghua Xiong, Xuesong Han: Conceived and designed the experiments, performed the experiments, analyzed and interpreted the data, wrote the paper.

Yaru Ma, Jia He: Conceived and designed the experiments, analyzed and interpreted the data.

Qin Li, Liu Liu, Chunli Yang: Performed the experiments.

Jia Chen, Yi Shen: Contributed reagents, materials, analysis tools or data.

Funding statement

This work was supported by the National Natural Science Foundation of China {81960269}, Yunnan Province "Ten Thousand People Plan" Famous Doctor Special Talent Project {RLHXS20210331}, and Yunnan Province Medical Leading Talent Project {L-2019005}.

Data availability statement

Data included in article/supplementary material/referenced in article.

Declaration of competing interest

The authors declare that they have no competing interests.

References

[1] R. Azizi, L. Aghebati-Maleki, M. Nouri, et al., Stem cell therapy in Asherman syndrome and thin endometrium: stem cell- based therapy, Biomed. Pharmacother. 102 (2018) 333–343.
[2] C.J. Lee, S.H. Hong, M.J. Yoon, et al., Eupatilin treatment inhibits transforming growth factor beta-induced endometrial fibrosis in vitro, Clin Exp Reprod Med 47 (2) (2020) 108–113.
[3] H. Lv, Z. Nan, P. Jiang, et al., Vascular endothelial growth factor 165 inhibits pro-fibrotic differentiation of stromal cells via the DLL4/Notch4/smad7 pathway, Cell Death Dis. 10 (9) (2019) 681.
[4] F. Xu, X. Shen, C. Sun, et al., The effect of mitomycin C on reducing endometrial fibrosis for intrauterine adhesion, Med Sci Monit 26 (2020), e920670.
[5] L. Liu, G. Chen, T. Chen, et al., si-SNHG5-FOXF2 inhibits TGF-β1-induced fibrosis in human primary endometrial stromal cells by the Wnt/β-catenin signalling pathway, Stem Cell Res. Ther. 11 (1) (2020) 479.
[6] F. Dai, P. Du, Y. Chang, et al., Downregulation of MiR-199b-5p inducing differentiation of bone-marrow mesenchymal stem cells (BMSCs) toward cardiomyocyte-like cells via HSF1/HSP70 pathway, Med Sci Monit 24 (2018) 2700–2710.
[7] H.L. Hang, Q. Xia, Role of BMSCs in liver regeneration and metastasis after hepatectomy, World J. Gastroenterol. 20 (1) (2014) 126–132.
[8] G. Wang, C. Ren, J. Jiang, Effects of bone marrow mesenchymal stem cells on repair and receptivity of damaged endometrium in rats, J. Obstet. Gynaecol. Res. 47 (9) (2021) 3223–3231.
[9] J. Yu, L. Jiang, Y. Gao, et al., Interaction between BMSCs and EPCs promotes IUA angiogenesis via modulating PI3K/Akt/Cox2 axis, Am J Transl Res 10 (12) (2018) 4280–4289.
[10] Q. Tan, D. Xia, X. Ying, miR-29a in exosomes from bone marrow mesenchymal stem cells inhibit fibrosis during endometrial repair of intrauterine adhesion, Int J Stem Cells 13 (3) (2020) 414–423.
[11] J.P. Santavanond, S.F. Rutter, G.K. Atkin-Smith, et al., Apoptotic bodies: mechanism of formation, isolation and functional relevance, Subcell. Biochem. 97 (2021) 61–88.
[12] L. Xin, C. Wei, X. Tong, et al., In situ delivery of apoptotic bodies derived from mesenchymal stem cells via a hyaluronic acid hydrogel: a therapy for intrauterine adhesions, Bioact. Mater. 12 (2022) 107–119.
[13] Q. Ma, M. Liang, Y. Wu, et al., Mature osteoclast-derived apoptotic bodies promote osteogenic differentiation via RANKL-mediated reverse signaling, J. Biol. Chem. 294 (29) (2019) 11240–11247.
[14] J. Liu, X. Qiu, Y. Lv, et al., Apoptotic bodies derived from mesenchymal stem cells promote cutaneous wound healing via regulating the functions of macrophages, Stem Cell Res. Ther. 11 (1) (2020) 507.

[15] I. Fatima, S. Barman, R. Rai, et al., Targeting Wnt signaling in endometrial cancer, Cancers 13 (10) (2021).
[16] S. He, S. Tang, WNT/β-catenin signaling in the development of liver cancers, Biomed. Pharmacother. 132 (2020), 110851.
[17] C. Kaloğlu, H.E. Bulut, R. Hamutoğlu, et al., Wingless ligands and beta-catenin expression in the rat endometrium: the role of Wnt3 and Wnt7a/beta-catenin pathway at the embryo-uterine interface, Mol. Reprod. Dev. 87 (11) (2020) 1159–1172.
[18] Y. Feng, Y. Li, M. Xu, et al., Bone marrow mesenchymal stem cells inhibit hepatic fibrosis via the AABR07028795.2/rno-miR-667-5p axis, Stem Cell Res. Ther. 13 (1) (2022) 375.
[19] X. Liu, S. Tan, H. Liu, et al., Hepatocyte-derived MASP1-enriched small extracellular vesicles activate HSCs to promote liver fibrosis, Hepatology 77 (4) (2023) 1181–1197.
[20] H. Kubo, Extracellular vesicles in lung disease, Chest 153 (1) (2018) 210–216.
[21] X. Shao, X. Wei, FOXP1 enhances fibrosis via activating Wnt/β-catenin signaling pathway in endometriosis, Am J Transl Res 10 (11) (2018) 3610–3618.
[22] L. Wang, D. Liu, J. Wei, et al., MiR-543 inhibits the migration and epithelial-to-mesenchymal transition of TGF-β-treated endometrial stromal cells via the MAPK and wnt/β-catenin signaling pathways, Pathol. Oncol. Res. 27 (2021), 1609761.
[23] N. Ebrahim, O. Mostafa, R.E. EL Dosoky, et al., Human mesenchymal stem cell-derived extracellular vesicles/estrogen combined therapy safely ameliorates experimentally induced intrauterine adhesions in a female rat model, Stem Cell Res. Ther. 9 (1) (2018) 175.
[24] M. Lodyga, B. Hinz, TGF-β1 - a truly transforming growth factor in fibrosis and immunity, Semin. Cell Dev. Biol. 101 (2020) 123–139.
[25] C.C. Gifford, J. Tang, A. Costello, et al., Negative regulators of TGF-β1 signaling in renal fibrosis; pathological mechanisms and novel therapeutic opportunities, Clin. Sci. (Lond.) 135 (2) (2021) 275–303.
[26] W. Qian, X. Cai, Q. Qian, et al., Astragaloside IV modulates TGF-β1-dependent epithelial-mesenchymal transition in bleomycin-induced pulmonary fibrosis, J. Cell Mol. Med. 22 (9) (2018) 4354–4365.
[27] X. Zhou, X.F. Yang, Progress of targeting transforming growth factor-β1 small interfering RNA in liver fibrosis, Chin. Med. Sci. J. 29 (4) (2014) 231–235.
[28] Y.Z. Huang, L. Zhao, Y. Zhu, et al., Interrupting TGF-β1/CCN2/integrin-α5β1 signaling alleviates high mechanical-stress caused chondrocyte fibrosis, Eur. Rev. Med. Pharmacol. Sci. 25 (3) (2021) 1233–1241.
[29] L. Yuan, J. Cao, M. Hu, et al., Bone marrow mesenchymal stem cells combined with estrogen synergistically promote endometrial regeneration and reverse EMT via Wnt/β-catenin signaling pathway, Reprod. Biol. Endocrinol.: RB&E 20 (1) (2022) 121.
[30] J. Wei, Y. Shan, Z. Xiao, et al., Anp32e promotes renal interstitial fibrosis by upregulating the expression of fibrosis-related proteins, Int. J. Biol. Sci. 18 (15) (2022) 5897–5912.
[31] D. Yuan, T. Guo, H. Qian, et al., Exosomal miR-543 derived from umbilical cord mesenchymal stem cells ameliorates endometrial fibrosis in intrauterine adhesion via downregulating N-cadherin, Placenta 131 (2023) 75–81.
[32] C.E. Gargett, L. Ye, Endometrial reconstruction from stem cells, Fertil. Steril. 98 (1) (2012) 11–20.
[33] J.C. Akers, D. Gonda, R. Kim, et al., Biogenesis of extracellular vesicles (EV): exosomes, microvesicles, retrovirus-like vesicles, and apoptotic bodies, Journal of neuro-oncology 113 (1) (2013) 1–11.
[34] Y. Yao, R. Chen, G. Wang, et al., Exosomes derived from mesenchymal stem cells reverse EMT via TGF-β1/Smad pathway and promote repair of damaged endometrium, Stem Cell Res. Ther. 10 (1) (2019) 225.
[35] H. Liu, S. Liu, X. Qiu, et al., Donor MSCs release apoptotic bodies to improve myocardial infarction via autophagy regulation in recipient cells, Autophagy 16 (12) (2020) 2140–2155.
[36] D. Liu, X. Kou, C. Chen, et al., Circulating apoptotic bodies maintain mesenchymal stem cell homeostasis and ameliorate osteopenia via transferring multiple cellular factors, Cell Res. 28 (9) (2018) 918–933.
[37] J. Miao, J. Liu, J. Niu, et al., Wnt/β-catenin/RAS signaling mediates age-related renal fibrosis and is associated with mitochondrial dysfunction, Aging Cell 18 (5) (2019), e13004.
[38] X. Li, T. Zhang, W. Lv, et al., Intratracheal administration of polystyrene microplastics induces pulmonary fibrosis by activating oxidative stress and Wnt/β-catenin signaling pathway in mice, Ecotoxicology and environmental safety 232 (2022), 113238.
[39] L. Shi, X. Xue, H. Tian, et al., WEE1 promotes endometriosis via the Wnt/β-catenin signaling pathway, Reprod. Biol. Endocrinol.: RB&E 19 (1) (2021) 161.
[40] Y. Guo, L. Xiao, L. Sun, et al., Wnt/beta-catenin signaling: a promising new target for fibrosis diseases, Physiol. Res. 61 (4) (2012) 337–346.